This paper is a condensation of a thesis which was submitted in partial fulfillment of the requirements for the degree of Master of chemical engineering by M. V. Hollander at New York University, New York, New York.

NOTATION

A = effective area, sq. cm.
c = concentration, counts/time, or moles/cc.
c' = concentration in lower reservoir, counts/time, or moles/cc.
c_1 = concentration in upper reservoir at time = t_1, counts/time, or moles/cc.
c_2 = concentration in upper reservoir at time = t_2, counts/time, or moles/cc.
D = diffusivity, sq. cm./sec.
L = thickness of diaphragm, cm.
t, t_1, t_2 = time, hours
V = volume of upper reservoir and circulation system, cc.
x = distance to any point in the diaphragm
μ = viscosity, centipoise

LITERATURE CITED

1. Bird, R. B., W. E. Stewart, and E. N. Lightfoot, "Transport Phenomena," pp. 513-515, Wiley, New York (1960).
2. Carslaw, H. S., and J. C. Jaeger, "Heat Conduction in Solids," 2 ed., pp. 59-60, Oxford University Press, New York (1959).
3. Gilliland, E. R., R. F. Baddour, and O. G. Goldstein, *Can. J. Chem. Eng.*, **35**, 10 (1957).
4. McBain, J. W., and T. H. Liu, *J. Am. Chem. Soc.*, **53**, 59 (1931).
5. McBain, J. W., and C. R. Dawson, *ibid.*, **56**, 52 (1934).
6. Northrop, J. H., and M. L. Anson, *J. Gen. Physiol.*, **12**, 543-57 (1929).

Manuscript received November 7, 1962; revision received January 30, 1963; paper accepted February 4, 1963.

Fluid Flow and Convective-Radiative Energy Transfer in a Parallel-Plate Channel Under Free-Molecule Conditions

E. M. SPARROW and V. K. JONSSON

University of Minnesota, Minneapolis, Minnesota

The flow of a highly rarefied gas in a parallel-plate channel and the transfer of heat owing to simultaneous thermal radiation and free-molecule convection has been investigated analytically. The analysis is facilitated by analogies which exist between the processes. The mass throughflow has been determined as a function of the temperatures and pressures of the system and of the channel dimensions. The heat transfer analysis is first carried out in general and then specialized to the boundary conditions of uniform wall temperature, uniform wall heat flux, and the adiabatic wall. It was found that at temperature levels corresponding to room temperature and above, the results for the combined convective-radiative transport differed little from those for a purely radiative transport.

This paper is concerned with the fluid flow and heat transfer characteristics of a highly-rarefied gas passing through a parallel-plate channel. The density level of the gas is such that collisions among molecules of the gas are much less probable than are collisions between the gas molecules and the bounding walls. This is called the *regime of free-molecule flow*. The very low gas density is effective in decreasing the convective energy transport, and as a consequence any complete analysis of the heat transfer must include the interchange of thermal radiation between the walls of the channel. Such an analysis including simultaneous convection and radiation is presented here. The relative importance of the two transport mechanisms will be carefully investigated.

The fluid-flow analysis will lead to a relationship between the mass flux through the channel and the pressures and temperatures at the inlet and exit. From the energy transport analysis, a relationship between wall temperature and wall heat transfer will be derived. The flow problem for the parallel-plate channel has been previously studied by DeMarcus (*1*) with a variational method. Comparison of his results with those of this analysis will be made later. Within the knowledge of the authors, the heat transfer problem for the parallel-plate channel has not been previously studied with or without radiation. It is the heat transfer problem which forms the larger part of this study.

The analysis to be reported here is facilitated by an analogy between the transport of mass and energy in a rarefied gas on one hand and the transport of thermal radiation on the other hand. This analogy is described in a general manner by Eckert (2). The specific application of the analogy to the free-molecule flow situation has been made in reference 3. There, consideration was given to flow and convective-energy transport (without radiation) in a circular tube. To assist in a concise presentation here, reference will be made to this prior work whenever possible.

A schematic diagram of the flow system is presented in Figure 1. The channel is of length L and of height h. The coordinate x measures the distance from the entrance. The channel connects two reservoirs which are of sufficient size so that thermal equilibrium exists within each. The left-hand reservoir has pressure and temperature p_1 and

T_1, while the right-hand reservoir has pressure and temperature p_2 and T_2. Pumps in an external circuit maintain the pressures at steady values. The reflection of mass and the emission and reflection of thermal radiation at the channel walls is assumed to be diffuse.

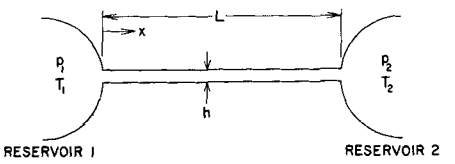

Fig. 1. Schematic of the physical system.

FLUID-FLOW ANALYSIS

For the condition of free-molecule flow, the molecules which originate in the left-hand reservoir and stream through the channel are unaware of the molecular stream from the right-hand reservoir. Therefore, each stream can be treated independently and the simultaneous effects of both streams can be found by linear superposition. Consideration will first be given to mass originating in the left-hand reservoir.

The flow problem is formulated by applying mass conservation at a typical location on the channel wall, say x_o, with area dA_{x_o}. The rate at which mass strikes x_o must be exactly equal to the rate at which mass streams away from x_o. The mass incident at x_o comes from two distinct zones: directly from the duct entrance, and by reflection from other locations on the duct wall. The mass flow per unit time and area entering the channel from reservoir 1 is

$$m_1 = p_1/\sqrt{2\pi RT_1} \tag{1}$$

This is uniformly and diffusely distributed across the channel entrance. Of this, an amount

$$m_1 \; F_{x_o-1} \tag{2a}$$

arrives per unit area at x_o. The quantity F is termed an angle factor (4). It represents the fraction of the diffusely distributed mass flux (or radiative flux) leaving one surface which arrives at a second surface.

Next, consider the mass arriving at x_o owing to interreflection. If $m(x)$ denotes the mass streaming away from a surface element at a location x per unit time and area, then $m(x)\, dF_{x_o-x}$ represents the amount of mass from location x which strikes per unit time and area at x_o. But mass arrives by interreflection at x_o from all surface locations $0 \leq x \leq L$ on the opposite channel wall and the total contribution is found by integration as

$$\int_{x=0}^{L} m(x)\, dF_{x_o-x} \tag{2b}$$

The sum of expressions (2a) and (2b) must equal the mass $m(x_o)$ streaming away from x_o per unit time and area. Introducing dimensionless variables, there follows

$$f(X_o) = F_{X_o-1} + \int_{X=0}^{1} f(X)\, dF_{X_o-X} \tag{3}$$

in which

$$f = m/m_1, \quad X = x/L \tag{4}$$

This is an integral equation, since the unknown f appears under the integral sign. The solution of Equation (4) gives, in dimensionless terms, the distribution of mass flux incident or leaving surface elements as a function of position along the length of the channel.

If the solution for $m(x)$ corresponding to mass streaming into the channel from the left-hand reservoir is $m_1 f(x)$, then from the symmetry of the situation, it is apparent that the $m(x)$ corresponding to mass streaming in from the right-hand reservoir is $m_2 f(L-x)$. The quantity m_2 is found by exchanging subscripts 2 for subscripts 1 in Equation (1). For the simultaneous action of both molecular streams, the $m(x)$ is

$$m(X) = \frac{p_1}{\sqrt{2\pi RT_1}} f(X) + \frac{p_2}{\sqrt{2\pi RT_2}} f(1-X) \tag{5}$$

This expression will be useful in the forthcoming heat transfer analysis.

The derivation of the mass flow through the channel is facilitated by first considering only the molecular stream owing to the left-hand reservoir 1. The net rate of mass throughflow is the difference between the mass streaming into the channel from reservoir 1 and that which returns to the reservoir as a result of reflections at the channel walls. The mass entering the channel from reservoir 1 per unit width normal to the plane of Figure 1 is $m_1 h$. Next, considering the back reflection, an amount $2m(x)F_{x-1}dx$ returns to reservoir 1 from locations x on both channel walls, and the mass returning from the entire channel length is simply the integral of this. If M represents the net rate of throughflow per unit channel width, then

$$M = m_1 h - 2\int_0^L m(x)F_{x-1}dx =$$

$$m_1 h\left[1 - 2\,(L/h)\int_0^1 f(X)F_{X-1}dx\right] \tag{6a}$$

where dimensionless variables have been introduced. The foregoing is owing to mass originating at the left-hand reservoir.

A similar expression applies for mass originating at the right-hand reservoir 2, except that m_1 is replaced by m_2 and F_{x-1} by F_{x-2}:

$$M = -\left[m_2 h - 2\int_0^L m(x)\, F_{x-2}dx\right] \tag{6b}$$

The negative sign is affixed because the latter mass throughflow is opposite in direction to that of Equation (6a). The $m(x)$ appearing in Equation (6b) may be replaced by $m_2 f(L-x)$. In addition, it is easy to show that

$$\int_0^L f(L-x)F_{x-2}dx = \int_0^L f(x)F_{x-1}dx$$

Thus Equation (6b) takes a form similar to the right-hand member of (6a) with the exception that $-m_2 h$ multiplies the bracket instead of $m_1 h$.

The net rate of mass throughflow owing to the simultaneous streams from both reservoirs is found by adding Equations (6a) and (6b), thus

$$\frac{M/h}{\frac{1}{\sqrt{2\pi R}}\left(\frac{p_1}{\sqrt{T_1}} - \frac{p_2}{\sqrt{T_2}}\right)} =$$

$$1 - 2(L/h)\int_0^1 f(X)\, F_{X-1}dX \tag{7}$$

The right side of this equation will be subsequently shown to depend only on the channel length-to-height ratio L/h. Therefore, Equation (7) embodies the dependence of the mass throughflow on the temperatures and pressures of the system and on the dimensions of the channel.

The key to the numerical evaluation of the mass throughflow is the function $f(X)$. It is necessary to solve

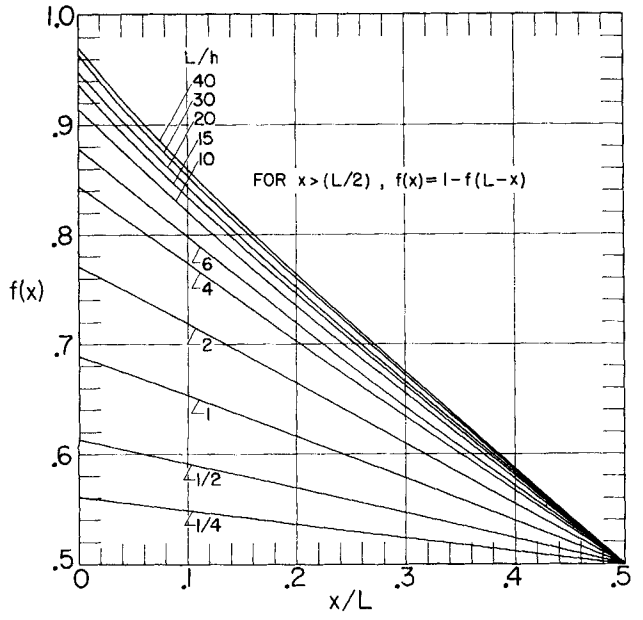

Fig. 2. The function f(x) for the mass flow problem.

Equation (3) to obtain f. As a prelude to these solutions, the angle factors F_{X_o-1} and dF_{X_o-X} are needed. These are available in the literature on thermal radiation as (for instance, reference 5)

$$F_{X_o-1} = \frac{1}{2}\left[1 - \frac{X_o}{X_o^2 + (h/L)^2}\right],$$

$$dF_{X_o-X} = \frac{\frac{1}{2}(h/L)^2\,dX}{[(X_o - X)^2 + (h/L)^2]^{3/2}} \qquad (8)$$

When the foregoing angle factors are considered, it is clear that the solution of Equation (3) will depend on a single parameter, L/h.

Exact analytical solutions cannot be obtained for Equation (3) and numerical means were employed instead. The numerical procedures are similar to those outlined in reference 3 and need not be repeated here. The $f(x)$ thus determined have been plotted in Figure 2. It may be observed that the abscissa covers the range from $x = 0$ to $x = 0.5L$. As noted on the figure, the f values for $0.5L < x \leq L$ are simply obtained as

$$f(x) = 1 - f(L - x) \qquad (9)$$

The proof of this property as given in the appendix of reference 3 also applies here for the parallel-plate channel. When it is recalled that f is proportional to the mass incident on the channel wall owing to the stream from reservoir 1, the curves of Figure 2 are physically plausible. For short channels, there is very little variation along the length; for long channels, there is substantial variation along the length. When the figure is carefully inspected, it is seen that the curves corresponding to small L/h are slightly concave downward, while those for large L/h are concave upward.

Utilizing these f solutions, the mass throughflow has been evaluated from Equation (7) and then plotted as a solid line in Figure 3 as a function of L/h. As expected, the figure shows that for fixed temperature and pressure conditions, the mass throughflow decreases with increasing channel length. The direction of mass flow is from the reservoir having the higher value of $p/\sqrt{T}$ to the reservoir having the lower value of $p/\sqrt{T}$. In particular, for isothermal conditions $T_1 = T_2$, the flow direction is from high to low pressure. On the other hand, when $p_1 = p_2$, the flow direction is from low to high temperature.

In the analysis by DeMarcus (*1*), the function corresponding to our f was approximated by a straight line, and the calculus of variations was employed to find the best straight line consistent with Equation (3). A straight line for f is seen to be in error (Figure 2) for the channels of large L/h. Notwithstanding this, the mass flow results derivable from DeMarcus's analysis agree quite well with the present results. To provide a simple computational formula for large L/h, the authors of this paper have derived an expression for M as an extension of DeMarcus's analysis and have taken the leading terms of this expression for large L/h. These are shown as a dashed line on Figure 3, from which it is concluded that $[\ln(2L/h) - 0.5]/(L/h)$ is a good approximation for the mass flow parameter for $L/h > 5$.

GENERAL ANALYSIS OF ENERGY TRANSPORT

A general formulation of the heat transfer problem encompassing arbitrary thermal boundary conditions will be carried out first. Later, consideration will be given to the cases of uniform wall temperature, uniform wall heat flux, and the adiabatic wall.

The net heat transfer q per unit time and area at some surface location is the sum of the separate contributions q_r and q_m owing respectively to the net radiation and to the net molecular convection:

$$q = q_r + q_m \qquad (10)$$

The quantities q, q_r, and q_m are all taken as positive when heat flows out of the surface. It is now necessary to relate q_r and q_m to the thermal and flow parameters of the system. These derivations are quite lengthy, and only a general outline will be given.

For the net radiative flux q_r at some location x_o (area dA_{x_o}) there are the following contributions to be considered: the emission, $\epsilon\sigma T^4(x_o)$, the radiation from reservoirs 1 and 2 which is directly incident and is absorbed at x_o, and the radiation from all other surface locations on the channel wall which arrives and is absorbed at x_o. Because there is thermal equilibrium in the reservoirs, the radiation streaming into the channel is blackbody radiation which is uniformly and diffusely distributed across the sections at $x = 0$ and $x = L$. From reservoir 1, an energy flux $\sigma T_1^4 F_{x_o-1}$ arrives at x_o per unit time and area; the corresponding quantity from reservoir 2 is $\sigma T_2^4 F_{x_o-2}$. Of these, a fraction α is absorbed. The absorbed energy flux owing to radiation leaving other surface locations requires a somewhat lengthy derivation which will be omitted here. When the various contributions to q_r are consolidated and gray-body conditions ($\epsilon = \alpha$) are assumed, one obtains

$$q_r(x_o) = \alpha\sigma T^4(x_o) - \alpha\sigma T_1^4 F_{x_o-1} - \alpha\sigma T_2^4 F_{x_o-2} -$$

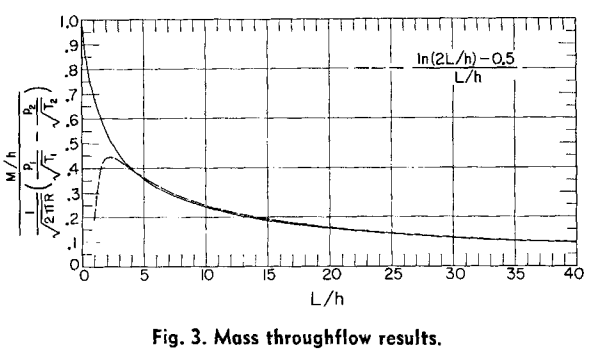

Fig. 3. Mass throughflow results.

$$\alpha\sigma\int_0^L T^4(x)\,dF_{x_o-x} + (1-\alpha)\int_0^L q_r(x)\,dF_{x_o-x} \tag{11}$$

The last terms on the right represent the energy absorbed at x_o owing to interreflected radiation.

The heat flux q_m for the molecular convection is most easily derived by analogy with the radiation balance of Equation (11). To accomplish this, it is necessary to introduce several new quantities. One of these is the accommodation coefficient* a, which characterizes the extent to which mass incident on a surface is brought into thermal equilibrium. In reference 3, it has been demonstrated that a plays a role in the convective transport analogous to that of α in the radiative transport. In addition, the black-body radiation from the reservoirs is analogous to the convective energy fluxes e_1 and e_2

$$e_{1,2} = 0.5\,R[(\gamma+1)/(\gamma-1)]\; m_{1,2}T_{1,2} \tag{12}$$

in which m_1 or m_2 may be found from Equation (1). Finally, the emissive power $\sigma T^4(x_o)$ at a surface location x_o is analogous to the equilibrium convective energy flux $e(x_o)$

$$e(x_o) = 0.5\,R[(\gamma+1)/(\gamma-1)]\,m(x_o)\,T(x_o) \tag{13}$$

The mass flux $m(x_o)$ has previously been derived and is represented by Equation (5). Utilizing the analogous quantities outlined above in conjunction with Equation (11), the convective energy balance is

$$q_m(x_o) = ae(x_o) - ae_1F_{x_o-1} - ae_2F_{x_o-2} - a\int_0^L e(x)\,dF_{x_o-x} + (1-a)\int_0^L q_m(x)\,dF_{x_o-x} \tag{14}$$

If the surface temperature is prescribed, then Equation (11) becomes an integral equation for determining q_r, and, for prescribed surface temperature, Equation (14) becomes an integral equation for q_m. Therefore, for this condition, Equations (11) and (14) are completely independent of one another. The separate solutions for q_r and q_m can be added together in accordance with Equation (10) and the local heat flux q corresponding to the prescribed surface temperature is thus obtained.

For the condition of prescribed heat flux, the problem is more complex. In general, although q might be prescribed, the separate radiative and molecular fluxes q_r and q_m would not be known a priori. Consequently, Equation (11) contains two unknowns: $T(x)$ and $q_r(x)$. Similarly, Equation (14) contains two unknowns: $T(x)$ and $q_m(x)$. It is therefore necessary to solve Equations (11) and (14) simultaneously in conjunction with Equation (10) and a prescribed distribution of q. The presence of three unknowns in the problem adds considerable complication as may be evidenced if one attempts to map out a procedure by which solutions may be obtained. It is possible, after a lengthy development, to reduce the foregoing mathematical problem to a single equation. Because of its length and complexity, this equation has been placed in the appendix as Equation (A1).

If $q(x)$ is prescribed, then in principle the temperature distribution $T(x)$ can be solved from Equation (A1). However, the practical details are quite formidable. First of all, the equation is nonlinear since the temperature appears both as T and T^4. Second, even in the relatively simple case of uniform wall heat flux $q(x) = q_o$, there would be seven independent parameters.

$$q_o/\sigma T_1^4;\quad T_2/T_1;\quad p_2/p_1;\quad \beta_1 = e_1/\sigma T_1^4;\quad L/h;\quad \alpha;\quad a \tag{15}$$

Of these, only the β_1 parameter may be somewhat unfamiliar and this will be discussed later. Inasmuch as numerical means would almost certainly be utilized in solving Equation (A1), it would be necessary to specify numerical values of the parameters before each attempt at a solution. A minimum exploration involving two values of each parameter would give rise to $2^7 = 128$ cases. Clearly, the computational effort for the general case is enormous.

For the special situation in which $a = \alpha$, a significant simplification occurs. For this condition, when Equations (11) and (14) are merged the heat transfer terms appear only as the sum $q_r + q_m = q$. Also, the temperature-dependent terms also appear only as a sum which will be denoted by

$$\theta = e + \sigma T^4 \tag{16}$$

With this, the sum of Equations (11) and (14) is

$$\frac{q(x_o)}{a} = \theta(x_o) - \theta_1F_{x_o-1} - \theta_2F_{x_o-2} - \int_0^L \theta(x)\,dF_{x_o-x} + (1-a)\int_0^L \frac{q(x)}{a}\,dF_{x_o-x} \tag{17}$$

It is seen that for a prescribed heat flux q, Equation (17) is linear in the temperature variable θ. The significance of this is that separate solutions can be found corresponding to each of the inhomogenous terms, and these can be consolidated at the end. This permits a subdivision of the problem into several parts with the result that the number of parameters involved in numerical solutions is drastically reduced. In addition, the linear equations are more amenable to numerical solution than are the nonlinear equations.

Discussion

In deciding on a reasonable direction for the numerical work, it is appropriate to look at the properties of typical engineering materials. Surfaces which may be expected to emit and reflect infrared radiation in an approximately diffuse manner include nonmetals, metallic oxides, and perhaps very rough metallic surfaces. Such surfaces have moderate or high values for the absorptivity coefficient α. Highly polished metallic surfaces are usually the specular type of reflectors, such as mirrors, and are characterized by low values of α, usually below 0.1. Therefore, an analytical model based on diffusely distributed radiation should be confined realistically to moderate or high α values. Furthermore, experimental values of the accommodation coefficient a tend to be high for various gases on engineering surfaces which have not been physically and chemically cleaned and purged of adsorbed gases. In the light of the foregoing discussion, it would appear that the values of α and a appropriate to an analysis based on diffusely distributed radiation should not be greatly different.

For the case of prescribed surface temperature, the heat fluxes owing to radiant transport and to free-molecule transport can be determined separately by solving Equations (11) and (14), respectively. The combined heat flux can then be found by summing these separate contributions. These calculations can be carried out for any α and a, but as described above they have practical meaning only for moderate and high values of α and a.

For the case of prescribed heat flux, it would be necessary to deal with Equation (A1) for the case of $\alpha \neq a$. When $\alpha = a$, then Equation (17) can be applied to the prescribed heat flux problem. In a first attack on any problem, it is natural to consider the simplest cases from which insights can be obtained about the physical process. When the foregoing discussion about the magnitudes

* Valuable discussions relating to the numerical values of a and their experimental determination are found in references 6 and 7.

of α and a is taken into account and the complexity of the mathematical system represented by Equation (A1) is recalled, the authors are persuaded that Equation (17) is a more appropriate starting point for numerical consideration than is Equation (A1). From the results to be presented in later sections, it will be seen that for surfaces which realistically can be considered as diffuse, there is little motivation to pursue the refinements (that is, $\alpha \neq a$) contained in Equation (A1).

It is appropriate here to say a few words about the parameter β_1 in Equation (15). In general, with subscript 1 removed, β denotes the ratio of the convective to the radiative energy flux. In particular, β_1 compares the convective and the radiative energy effluxes from reservoir 1. As employed in the forthcoming presentation, β_1 will be a multiplying factor of the convective terms in the heat transfer or temperature equations. For air at 500°R. (room temperature), $\beta = 10^5\ p$ (atm.). For a plate spacing of 0.1 in. pressures no greater than 2 μ mercury (2.6×10^{-6} atm.) would probably insure free-molecule conditions; while for a spacing of 1 in., pressures of 0.2 μ mercury and less would be required.* The corresponding room temperature β values would be 0.26 and 0.026. Since $\beta \sim T^{-3.5}$, it is seen that β becomes larger at low temperatures and becomes smaller at high temperatures.

UNIFORM WALL TEMPERATURE

For the condition that $T(x) = T_o = a$ constant, the governing Equation (11) for q_r becomes

$$\frac{q_r(x_o)}{\alpha} = \sigma\,(T_o^4 - T_1^4)\,F_{x_o-1} + \sigma\,(T_o^4 - T_2^4)\,F_{x_o-2} + (1-\alpha)\int_o^L \frac{q_r(x)}{\alpha}\,dF_{x_o-x} \quad (18)$$

A similar reduction of Equation (14) leads to

$$\frac{q_m(x_o)}{a} = e_1\left(\frac{T_o}{T_1} - 1\right)F_{x_o-1} + e_2\left(\frac{T_o}{T_2} - 1\right)F_{x_o-2} + (1-a)\int_o^L \frac{q_m(x)}{a}\,dF_{x_o-x} \quad (19)$$

The solution of these is facilitated by considering the integral equation

$$g_i(X_o) = F_{X_o-1} + (1-i)\int_o^1 g_i(X)\,dF_{X_o-X},\quad i = a \text{ or } \alpha \quad (20)$$

In terms of the g function, q_r can be written as

$$q_r(X)/\alpha = \sigma\,(T_o^4 - T_1^4)\,g_\alpha(X) + \sigma\,(T_o^4 - T_2^4)\,g_\alpha(1-X) \quad (21)$$

A similar result applies for q_m. The local heat flux q is then found as the sum of q_r and q_m as

$$q(X)/\sigma T_1^4 = \alpha\left\{\left[\left(\frac{T_o}{T_1}\right)^4 - 1\right]g_\alpha(X) + \left[\left(\frac{T_o}{T_2}\right)^4 - 1\right]\left(\frac{T_2}{T_1}\right)^4 g_\alpha(1-X)\right\} + a\beta_1\left\{\left(\frac{T_o}{T_1} - 1\right)g_a(X) + \left(\frac{T_o}{T_2} - 1\right)\frac{p_2}{p_1}\sqrt{\frac{T_2}{T_1}}\,g_\alpha(1-X)\right\} \quad (22)$$

* Ratio of mean free path to spacing is 10.

In addition to the local heat flux, it is also of interest to determine the rate Q (per unit width) at which heat is transferred from the entire length of channel:

$$Q = 2\int_o^L q(x)\,dx \quad (23)$$

When the result for q as given by Equation (22) is utilized, there follows

$$\frac{Q}{2\sigma T_1^4 h} = \alpha I_\alpha\left[2\left(\frac{T_o}{T_1}\right)^4 - \left(\frac{T_2}{T_1}\right)^4 - 1\right] + a\beta_1 I_a\left[\left(\frac{T_o}{T_1} - 1\right) + \left(\frac{T_o}{T_2} - 1\right)\frac{p_2}{p_1}\sqrt{\frac{T_2}{T_1}}\right] \quad (24)$$

in which

$$I_i \cdot (h/L) = \int_o^1 g_i(X)\,dX = \int_o^1 g_i(1-X)\,dX \quad (25)$$

To complete the heat transfer results, it still remains to provide the g function and its integral I. This information has been obtained by numerically solving the integral Equation (20) for parametric values of L/h of 0.25, 0.50, 1, 2, 4, 6, 10, 15, 20, 30, and 40. For each one of these, solutions were carried out for a and α values of 1.0, 0.8, 0.6, 0.4, and 0.2. A presentation of the solutions for g as a function of x would involve a set of graphs containing fifty-five curves. This is precluded by space limitations; however, the graphs are available and may be obtained from the authors.

In general, a typical graph would show that g decreases with x. For short ducts, the g function varies only slightly with position along the channel. Correspondingly, the local heat flux q undergoes only a modest variation with position. As L/h increases, so does the variation of g with x. For very long ducts, both $g(x)$ and $g(L-x)$ are essentially zero in the central region of the channel. Because of this, the local heat flux q in the central region of long channels is also essentially zero. This is physically plausible inasmuch as neither radiant energy nor molecular convection can penetrate very far in from the ends of the channel. The g curves lie lower with increasing values of a or α. However, the effect of this on the local heat flux q is opposed by the factors of a and α which appear in Equation (22).

The I integral needed for the overall heat transfer results have been calculated in accordance with Equation (25). In general, a graph of I as a function of L/h increases sharply from a value of zero at $L/h = 0$ and then tends to level off at larger L/h. Indeed, the most striking feature of such a graph is that I is relatively independent of L/h in the range of larger L/h, especially at the moderate or higher values of a or α. When Equation (24) is considered, this feature implies that Q is relatively independent of L/h except for short channels. For instance, when a and α are on the order of 0.6 and larger, the overall heat transfer rate for a channel of $L/h = 40$ is less than 2% greater than that for a channel of $L/h = 20$. Once again, space limitations preclude graphical presentation of the I function, but for purposes of orientation it may be noted that the I values at $L/h = 40$ are 0.493, 0.587, 0.732, 0.990, and 1.631 respectively for a or α = 1.0, 0.8, 0.6, 0.4, and 0.2.

With the aforementioned information at hand, the local and overall heat transfer rates can be respectively calculated from Equations (22) and (24) by simple arithmetic operations. These results depend upon seven independent parameters

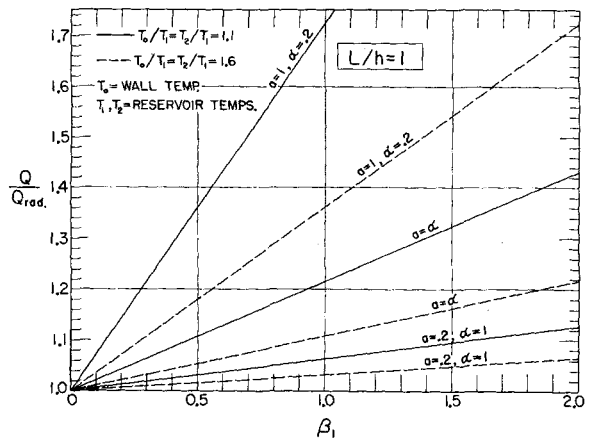

Fig. 4a. Illustrative heat transfer results for uniform wall temperature, $L/h = 1$.

$$T_o/T_1;\ T_2/T_1;\ p_2/p_1;\ L/h;\ \beta_1;\ \alpha;\ a$$

For the local heat flux, the position coordinate x/L is another variable. In any reasonable amount of space, it is impossible to present plots which will demonstrate the complete parametric dependence of the heat transfer. Within the limitations of space, the best that can be done is to attempt to establish some feeling for trends. To this end, Figures 4*a* and 4*b* have been constructed. These deal with the overall heat transfer results for some representative situations. (The overall heat transfer permits a simpler presentation than the local heat transfer because the x-dependence does not appear.)

Figure 4*a* is meant to typify short channels, while Figure 4*b* is to typify long channels. On the ordinate, the heat transfer Q is plotted as a ratio with the heat transfer Q_{rad} for purely radiative transport. The departure of Q/Q_{rad} from unity is a direct measure of the effects of molecular convection. Curves are shown for two temperature conditions, $T_o/T_1 = 1.1$ (solid lines) and $T_o/T_1 = 1.6$ (dashed lines), and for a variety of α and a values. From the figures, it is seen that for small values of β_1 radiation is apparently the more important mode of heat transfer. As previously noted, representative β_1 values for air at 500°R. may be in the range 0.026 to 0.26. Further, since $\beta_1 \sim T_1^{-3.5}$, it appears that radiation will dominate at temperature levels above room temperature. At lower temperatures, molecular convection will have a more important effect.

For the short channel (Figure 4*a*), the detailed values of the temperature ratio and of the surface properties have an important influence on the Q/Q_{rad} ratio. Surfaces having an accommodation coefficient much higher than the absorptivity favor the molecular convection. When $\alpha = a$ and particularly when $\alpha > a$, the molecular convection plays a decidedly minor role. It is also seen from the figure that the radiation dominates more fully when the temperature ratios of the problem are larger.

The results for the long channel (Figure 4*b*) show some interesting differences in detail compared with those for the short channel. First of all, the molecular convection is clearly of lesser importance in the long channel. Second, the results are much less influenced by the detailed values of α and a. This is physically plausible, since the multireflections which take place in a long channel produce effective values of α or a which are much higher than the actual values. The relative insensitivity just noted means that the $\alpha = a$ results become fairly typical for a channel of given L/h and temperature ratio. It may also be noted that channels of moderate length already behave like long channels.

UNIFORM WALL HEAT FLUX

As previously discussed, the uniform heat flux case will be treated here for the condition of $a = \alpha$. Returning to Equation (17) and introducing $q(x) = q_o$ = constant, there follows after some rearrangement

$$\theta(X_o) = q_o + \left[\theta_1 + \frac{1-a}{a} q_o\right] F_{X_o-1} + \left[\theta_2 + \frac{1-a}{a} q_o\right] F_{X_o-2} + \int_o^1 \theta(X)\, dF_{X_o-X} \quad (26)$$

When solutions of this equation are considered, it is helpful to make use of the auxiliary integral equation

$$H(X_o) = 1 + \int_o^1 H(X)\, dF_{X_o-X} \quad (27)$$

The solution corresponding to the inhomogeneous part q_o of Equation (26) can be written in terms of the H function, while the solutions corresponding to the inhomogeneous terms involving F_{X_o-1} and F_{X_o-2} can be written in terms of the f function of Equation (3). With these, the solution for θ is

$$\theta(X) = e(X) + \sigma T^4(X) = \theta_1 f(X) + \theta_2 f(1-X) + q_o\left[\frac{1-a}{a} + H(X)\right] \quad (28)$$

in which Equation (9) has also been used. When the definitions of θ and e are introduced and the equation is rearranged, there follows

$$\left[\frac{T(X)}{T_1}\right]^4 + \beta_1\left[f(X) + \frac{p_2}{p_1}\sqrt{\frac{T_1}{T_2}} f(1-X)\right] \frac{T(X)}{T_1} = (1+\beta_1) f(X) + f(1-X)\left[\beta_1 \frac{p_2}{p_1}\sqrt{\frac{T_2}{T_1}} + \left(\frac{T_2}{T_1}\right)^4\right] + \frac{q_o}{\sigma T_1^4}\left[\frac{1-a}{a} + H(X)\right] \quad (29)$$

This is a fourth degree algebraic equation for the distribution of the wall temperature as a function of position along the channel. The calculation requires the functions f and H as input data. The first of these has already been discussed and is plotted in Figure 2. The H function has been solved numerically, but space limitations preclude its presentation here. In general, a graph of H as a function of x would increase monotonically from a nonzero value at $x = 0$ to a maximum at $x = 0.5L$. Such a graph would be symmetric about $x = 0.5L$. For channels with

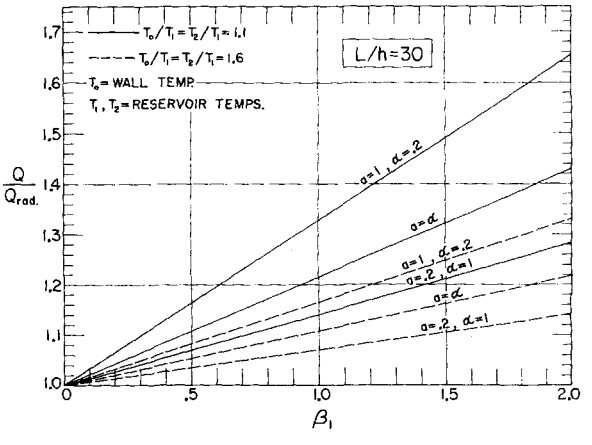

Fig. 4b. Illustrative heat transfer results for uniform wall temperature, $L/h = 30$.

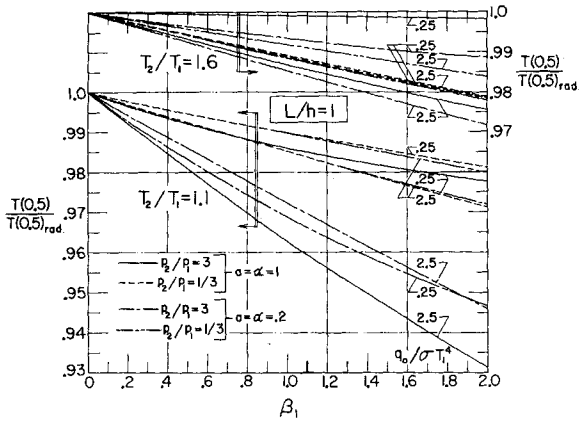

Fig. 5a. Illustrative wall temperatures for uniform heat flux, $L/h = 1$.

large L/h, the H function takes on large values, especially in the central region of the channel. Thus, at $x/L = 0.5$, H has the values 1.14, 1.32, 1.77, 2.93, 5.92, 9.62, 18.9, 33.8, 52.0, 97.7, and 155.3 respectively for aspect ratios L/h of 0.25, 0.5, 1, 2, 4, 6, 10, 15, 20, 30, and 40.

With the f and H functions thus available, the variation of the wall temperature along the length of the channel can be determined from Equation (29). Solutions of the quartic can be obtained in closed form by finding the roots of the resolvent cubic as described in reference 8. The wall temperature results depend upon the values of six independent parameters as listed in Equation (15) with $\alpha = a$. Once again, space limitations preclude a display of the complete parametric dependence of the results. To show the trends, the illustrative Figures 5*a* and 5*b* have been prepared. The first of these, for $L/h = 1$, is meant to typify a short channel, while the latter is for a typically long channel, $L/h = 30$. On the ordinate, there is plotted the ratio of the wall temperature at some x location to the wall temperature which would exist at the same x when radiation acts alone. The departure of the T/T_{rad} ratio from unity is a direct measure of the effects of free-molecule convection. Curves are plotted for pressure ratios p_2/p_1 of 3 and 1/3, temperature ratios T_2/T_1 of 1.1 and 1.6, and $q_o/\sigma T_1^4$ values of 0.25 and 2.5.

Consideration is first given to Figure 5*a* on which is shown the T/T_{rad} results at $x = 0.5L$. From auxiliary plots, it was found that the T/T_{rad} ratio at other x positions did not differ qualitatively from those of Figure 5*a*. This is quite reasonable for a short channel. The most striking feature of this figure is the highly expanded ordinate scale. For the previously estimated room-temperature values of $\beta_1 \sim 0.026 - 0.26$, it would appear that the effect of molecular convection is essentially negligible for all the cases considered in the figure. Even for the large β_1 values, the departures of T from T_{rad} continue to be small. The largest departures occur for $p_2/p_1 = 3$. However, since $\beta_1 \sim p_1$, it is not likely that large β_1 and large p_2/p_1 will occur simultaneously. The results for $T_2/T_1 = 1.6$, plotted at the top of the figure, show a smaller effect of molecular convection than do the results for $T_2/T_1 = 1.1$ which are plotted at the lower part of the figure. It is also seen that the curves are somewhat affected by the values of $q_o/\sigma T_1^4$ and α $(= a)$. Although T and T_{rad} vary in a regular way with these parameters, the ratio T/T_{rad} need not, and this is evidenced in Figure 5*a*.

The results shown in Figure 5*a* were calculated for the condition $\alpha = a$. When $\alpha > a$, the deviations of T/T_{rad} from unity should be even smaller than those of the figure. On the other hand, when $a > \alpha$, the deviations from unity will be larger than those of the figure. However, it is the opinion of the authors that radiation will still be the dominant transfer mechanism at typical β_1 (that is, $\beta_1 \sim 0.026 - 0.26$) even if a is much greater than α. When a is only moderately larger than α, the T/T_{rad} results should differ little from those of the figure.

Next, consideration is given to the results typical of long channels, Figure 5*b*. The T/T_{rad} ratios are now a stronger function of position than for the short channel. In accordance with this, results are plotted for $x/L = 0$, 0.5, and 1, the first of these on the lower part of the figure and the latter two on the upper part of the figure. Highly expanded ordinate scales are used as before. The most interesting feature of this figure is that the results are essentially independent of the level of α (or a). In general, radiation appears to dominate in about the same way as was discussed in connection with Figure 5*a*.

For long ducts, it is expected that the detailed values of a or α will have no significant effect on the results within the range of a or α in which the diffuse assumption is reasonable.* In other words, the results for $\alpha = a$ should be applicable with negligible error for long channels. Thus, Equation (29) can be applied quite generally for long channels and the term $(1 - a)/a$ may be deleted without loss. An estimate of the conditions under which the aforementioned long-channel generalization applies may be found by comparing $(1 - a)/a$ or $(1 - \alpha)/\alpha$ with $H(x)$.

THE ADIABATIC WALL

The analysis for the adiabatic wall is most easily carried out as a special case of uniform heat flux in which $q_o = 0$. Further, when $\alpha = a$, the solution for the adiabatic wall temperature follows from Equation (29) simply by deleting the last term on the right-hand side of the equation. The calculation of numerical results depends upon the f function (available from Figure 2) and upon the values of four independent parameters: T_2/T_1, p_2/p_1, L/h, and β_1. There is also a dependence on the position coordinate x. As before, space limitations restrict the graphical presentation of results to illustrative cases.

Figure 6 contains adiabatic wall temperature results for a typical short channel, $L/h = 1$, at three locations: $x/L = 0$, 0.5, and 1. The ordinate is the ratio of the adiabatic wall temperature at a given location to the adiabatic wall temperature for pure radiative transport at the same location. Curves are plotted for various pres-

* For very low α or a, it would be expected that the directional properties of the reflection would be closer to specular.

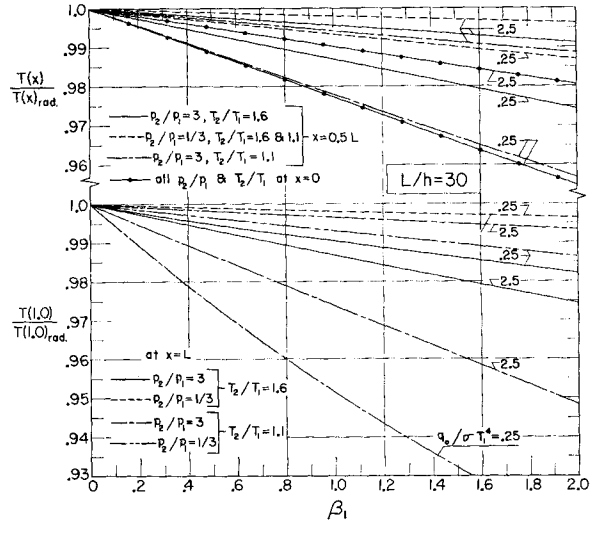

Fig. 5b. Illustrative wall temperatures for uniform heat flux, $L/h = 30$.

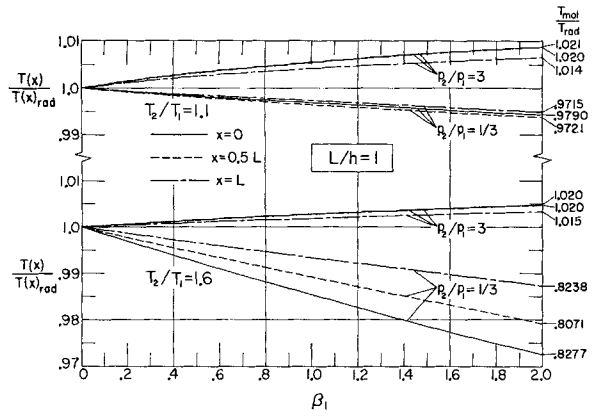

Fig. 6. Illustrative adiabatic wall temperatures, $L/h = 1$.

sure and temperature ratios. The upper part of the figure is for $T_2/T_1 = 1.1$, while the lower part of the figure is for $T_2/T_1 = 1.6$. When the figure is inspected, it is immediately evident that the deviations of T from T_{rad} are very small indeed. In fact, for $\beta_1 \sim 0.25$, the deviations do not exceed one-half of 1%. From this, one might be led to conclude that radiation is fully dominant over free-molecule convection. This is not necessarily the case. To demonstrate this, the adiabatic wall temperature corresponding to pure molecular convection, T_{mol}, has been calculated and is noted in the right-hand margin of the figure as a ratio T_{mol}/T_{rad}. In many cases T_{mol}/T_{rad} is not very different from unity. However, the essential point is that when T_{mol} and T_{rad} are appreciably different, it is the radiative transport which wins out.

The results for a typical long tube can be described without the use of an additional figure. At locations near the entrance and exit of the channel, T_{rad} and T_{mol} are not very different. Therefore, the adiabatic wall temperature caused by the simultaneous operation of both mechanisms will differ little from either T_{mol} or T_{rad}. For the central region, $x = 0.5L$, the dashed curves of Figure 6 continue to apply for any channel L/h. As before, when T_{mol} and T_{rad} are significantly different, the radiative transport dominates.

It appears quite clear that for the case when α and a are not very different, the adiabatic wall temperature can be calculated without appreciable error by considering only the radiative transport. The authors believe that this conclusion will continue in force for moderate β_1 values for any a and α which are consistent with the assumption of diffuse reflection.

NOTATION

A = surface area
a = accommodation coefficient
e = convective energy/time-area
F = angle factor
$f(x)$ = solution of Equation (3)
$g(x)$ = solution of Equation (20)
$H(x)$ = solution of Equation (27)
h = spacing between plates
I = integral of g function, Equation (25)
L = channel length
M = rate of mass throughflow
m = mass flux/time-area
p = pressure
Q = overall heat flux/time
q = local heat flux/time-area
q_o = uniform heat flux
R = gas constant
T = absolute temperature
T_o = uniform wall temperature
X = dimensionless coordinate, x/L
x = longitudinal coordinate
x_o = a particular value of x

Greek Letters

α = absorptivity
β = ratio of convective to radiative energy efflux
γ = specific heat ratio
ϵ = emissivity
θ = energy variable, Equation (16)
ρ = reflectivity
σ = Stefan-Boltzmann constant

Subscripts

1 = reservoir 1
2 = reservoir 2
i = a or α
r, rad = radiative
m, mol = molecular

LITERATURE CITED

1. DeMarcus, W. C., *Report K-1302*, Union Carbide Nuclear Company, Oak Ridge Gaseous Diffusion Plant, Oak Ridge, Tennessee (March, 1957).
2. Eckert, E. R. G., "Modern Developments in Heat Transfer," W. E. Ibele, ed., pp. 159-180, Academic Press, New York (1963).
3. Sparrow, E. M., V. K. Jonsson, and T. S. Lundgren, *Heat Transfer*, **85**, 111-118 (1963).
4. Jakob, Max, "Heat Transfer," Vol. 2, Wiley, New York (1957).
5. Sparrow, E. M., J. L. Gregg, J. V. Szel, and P. Manos, *Heat Transfer*, 83, 207-214 (1961).
6. Hartnett, J. P., "Advances in Applied Mechanics," Supplement 1, Rarefied Gas Dynamics, pp. 1-28, Academic Press, New York (1961).
7. Wachman, H. Y., *Am. Rocket Soc. J.*, **32**, 2-12 (1962).
8. Burington, R. S., "Handbook of Mathematical Tables and Formulas," pp. 8-9, Handbook Publishers, Sandusky, Ohio (1940).

Manuscript received November 1, 1962; revision received February 4, 1963; paper accepted February 6, 1963.

APENDIX

General Integral Equation Relating T(x) and q(x)

$$-q(X_o) + \alpha\sigma T^4(X_o) + ae(X_o) - \Lambda(X_o) =$$

$$\sigma\int_o^1 T^4(X)[\alpha(2-a)dF_{X_o-X} - \alpha(1-a)dK(X, X_o)]$$

$$+\int_o^1 e(X)[a(2-\alpha)dF_{X_o-X} - a(1-\alpha)dK(X, X_o)]$$

$$-\int_o^1 q(X)\{[(1-a) + (1-\alpha)]dF_{X_o-X} - (1-a)(1-\alpha)dK(X, X_o)\} \quad (A1)$$

$\Lambda(X)$ represents a known function of X

$$\Lambda(X_o) = [\alpha\sigma T_2^4 + ae_2]F_{X_o-2} - [\alpha(1-a)\sigma T_2^4 + a(1-\alpha)e_2]\int_o^1 F_{X-2}dF_{X_o-X} + [\alpha\sigma T_1^4 + ae_1]F_{X_o-1} - [\alpha(1-a)\sigma T_1^4 + a(1-\alpha)e_1]\int_o^1 F_{X-1}dF_{X_o-X}$$

and dK is an abbreviation for

$$dK(X, X_o) = \int_{X^1=0}^1 dF_{X^1-X}dF_{X_o-X^1}$$

with X^1 a dummy integration variable.